

Diffusion-Modeled Reinforcement Learning for Carbon and Risk-Aware Microgrid Optimization

Yunyi Zhao, *Student Member, IEEE*, Wei Zhang, *Member, IEEE*, Cheng Xiang, *Member, IEEE*, Hongyang Du, *Member, IEEE*, Dusit Niyato, *Fellow, IEEE*, and Shuhua Gao, *Member, IEEE*

Abstract—This paper introduces DIFFCARL, a diffusion-modeled carbon- and risk-aware reinforcement learning algorithm for intelligent operation of multi-microgrid systems. With the growing integration of renewables and increasing system complexity, microgrid communities face significant challenges in real-time energy scheduling and optimization under uncertainty. DIFFCARL integrates a diffusion model into a deep reinforcement learning (DRL) framework to enable adaptive energy scheduling under uncertainty and explicitly account for carbon emissions and operational risk. By learning action distributions through a denoising generation process, DIFFCARL enhances DRL policy expressiveness and enables carbon- and risk-aware scheduling in dynamic and uncertain microgrid environments. Extensive experimental studies demonstrate that it outperforms classic algorithms and state-of-the-art DRL solutions, with 2.3–30.1% lower operational cost. It also achieves 28.7% lower carbon emissions than those of its carbon-unaware variant and reduces performance variability. These results highlight DIFFCARL as a practical and forward-looking solution. Its flexible design allows efficient adaptation to different system configurations and objectives to support real-world deployment in evolving energy systems.

Index Terms—Diffusion models, generative artificial intelligence, multi-microgrids, carbon aware, energy scheduling, risk-sensitive, deep reinforcement learning

I. INTRODUCTION

IN recent years, microgrids have gained increasing attention in many nations with increasing utilization of renewable energy sources as substitutes of traditional fossil energy. Such transition not only brings economic benefits but also contributes to environmental sustainability by reducing emissions

Manuscript received January 1, 2025; revised January 1, 2025; accepted January 1, 2025. This research was supported in part by MTC Individual Research Grants (IRG) (Award M23M6c0113), A*STAR under its MTC Programmatic (Award M23L9b0052), and the National Research Foundation Singapore and DSO National Laboratories under the AI Singapore Programme (AISG Award No: AISG2-GC-2023-006). (*Corresponding author: Wei Zhang*)

Yunyi Zhao is with both the Information and Communications Technology Cluster, Singapore Institute of Technology, Singapore 138683, and the Department of Electrical and Computer Engineering, National University of Singapore, Singapore 119077 (e-mail: yunyi.zhao@singaporetech.edu.sg).

Wei Zhang is with the Information and Communications Technology Cluster, Singapore Institute of Technology, Singapore 138683 (e-mail: wei.zhang@singaporetech.edu.sg).

Cheng Xiang is with the Department of Electrical and Computer Engineering, National University of Singapore, Singapore 119077 (e-mail: elexc@nus.edu.sg).

Hongyang Du is with the Department of Electrical and Electronic Engineering, University of Hong Kong, Hong Kong SAR, China (e-mail: duhy@eee.hku.hk).

Dusit Niyato is with the College of Computing and Data Science, Nanyang Technological University, Singapore 639798 (e-mail: dniyato@ntu.edu.sg).

Shuhua Gao is with the School of Control Science and Engineering, Shandong University, Jinan, China (e-mail: shuhua.gao@sdu.edu.cn).

of carbon dioxide and other greenhouse gases. Microgrids adopt a localized and decentralized approach to manage energy with higher resilience and flexibility than traditional centralized grids. In addition to renewable distributed generation (RDG), microgrids often integrate energy storage systems (ESS), controllable diesel generation (CDG), and loads. While conventional microgrids typically involve control within a bounded system, recent developments have expanded this concept. The notion of a microgrid community (MGC) [1] has been introduced to represent decentralized and cooperative energy systems that span multiple microgrids for achieving collective energy scheduling and optimization goals.

At the system level, the goal of operating microgrids and MGC is to maximize efficiency, reduce costs, and minimize environmental impact while ensuring stability and reliability. Practical energy scheduling faces key challenges, including the uncertainty of renewable generation, demand variability, and coordination of heterogeneous components under constraints like limited communication and decentralized control. Operational limits, such as ramping rates, storage state-of-charge, and network constraints, add non-linearity and complicate real-time optimization [2]. In large-scale MGC, the growing number of decision variables and amplified uncertainty further increase complexity, making effective inter-microgrid coordination essential. These challenges demand robust, scalable, and adaptive solutions responsive to dynamic conditions.

Numerous studies have addressed energy scheduling and optimization in microgrids. Early approaches formulated the problem as mixed-integer nonlinear programming (MINLP) [3] or as mixed-integer linear programming (MILP) with linearization for tractability [4], [5]. To incorporate real-time information, model predictive control (MPC) was introduced as an extension of MILP-based frameworks [6], [7], offering some robustness but still limited to single or centralized microgrids. To improve scalability, hierarchical and distributed frameworks have been proposed, such as a two-level hierarchical MILP for negotiation among agents [8] and a distributed MILP for coordinating interconnected microgrids [9]. Despite these advances, numerical optimization remains computationally expensive and relies on accurate predictions of renewables, loads, and markets, which is a significant challenge in practice.

Recently, data-driven machine learning (ML), particularly deep reinforcement learning (DRL), has been explored to improve optimization performance and efficiency. The problem is often cast as a Markov decision process (MDP), where agents learn near-optimal policies by interacting with the environ-

ment, avoiding the need for precise forecasts. DRL has shown fast convergence and strong performance in applications like battery operation optimization, demand response, and energy management [10], [11]. However, early value-based methods like Q-learning and DQN struggle with the large state and action spaces typical in microgrids. To address this, imitation learning (IL) has been used to leverage expert demonstrations for faster training and near-optimality [12]–[14], but suffers from overfitting and distributional shift due to reliance on expert policy quality [15]. More advanced methods such as DDPG [16], SAC [17], PPO [18], and TD3 [19] have since been developed.

Despite these advances, energy scheduling in microgrid clusters (MGC) remains challenging due to dynamic environments, combinatorial action spaces, and multi-agent coordination. Recently, generative AI (GenAI) has emerged as a promising approach, enhancing robustness, interpretability, and adaptability under uncertainty. GenAI shifts from deterministic to probabilistic and adaptive decision-making, augmenting DRL by modeling distributions over actions rather than fixed policies. Its ability to emulate experts while generalizing to novel conditions makes it a valuable tool for intelligent energy scheduling. In [20], GenAI integrated with SAC improved performance in a non-energy domain. In [21], a GenAI-based DRL algorithm for multi-energy scheduling was proposed but still derived a deterministic policy, limiting robustness under high uncertainty. These limitations underscore the need to further improve GenAI-based approaches for reliable scheduling in complex energy systems.

In this paper, we leverage the strength of GenAI and improve DRL for MGC energy scheduling and optimization. By formulating decision-making as a denoising generation process, diffusion policies offer both diversity and constraint-awareness, making them well-suited for dynamic, uncertain, and real-time energy environments. We propose DIFFCARL: diffusion-modeled carbon and risk-Aware Reinforcement learning, a novel framework that addresses key limitations in existing solutions in two main aspects. First, DIFFCARL leverages diffusion modeling to learn expressive and flexible policies capable of handling complex MGC dynamics and outperforming conventional DRL algorithms. Second, unlike many traditional solutions focusing solely on minimizing energy cost, DIFFCARL explicitly incorporates carbon intensity and operational risk into its decision-making. This integrated design is driven by the practical need for sustainable and resilient microgrids, where operations shall align with decarbonization goals and safety-critical constraints. Overall, DIFFCARL is a practical and forward-looking solution for energy scheduling under increasing system complexity and uncertainty. The main contributions of this paper are summarized as follows.

- 1) We formulate an energy scheduling and optimization problem and an interactive learning environment for MGC, explicitly incorporating carbon emission and operational risks into the formulation.
- 2) We propose DIFFCARL algorithm, which integrates diffusion model in DRL to optimize MGC energy schedules with improved performance in spite of the uncertainty

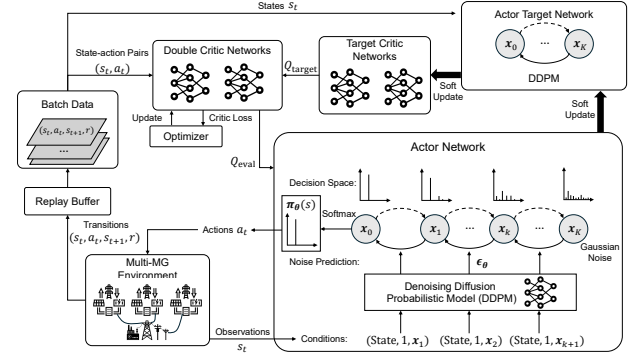


Fig. 1: The framework of DIFFCARL with diffusion-modeled actor network.

of renewable, loads, and the market.

- 3) We apply carbon- and risk-awareness to DIFFCARL algorithm, which effectively minimizes carbon emission and reduces the risk of high operational cost, thereby satisfying the user’s need of balancing cost efficiency, sustainability and manageable risk exposure.
- 4) We conduct extensive experiments to evaluate the performance of DIFFCARL. The results show that DIFFCARL achieves lower operational cost, less carbon emission and better risk management compared with several classic and state-of-the-art DRL algorithms.

The remainder of this paper is organized as follows. Section II details the system architecture and the proposed algorithm DIFFCARL. Section III reports the simulation studies and provides a comprehensive discussion. Finally, Section IV concludes the paper.

II. METHODOLOGY

In this paper, we consider a classic microgrid cost minimization problem [6], [8], [12] and incorporate carbon-awareness into a MILP-based optimization problem. Typically, a classic microgrid model consists of controllable distributed generators (CDGs), non-controllable renewable distributed generators (RDGs), and energy storage systems (ESSs); generally, the microgrids’ power is exchangeable with the utility grid (UG) in the grid-connected mode and nonexchangeable in the islanded mode. Afterwards, we work on combining generative models in reinforcement learning (RL). Traditional RL is inefficient in real-world applications due to its slow convergence and is vulnerable to overestimation and risks in real world applications. In this section, we aim to solve the formulated optimization problem for MGC energy management and we present our proposed algorithm DIFFCARL. DIFFCARL is a diffusion model-based DRL algorithm which follows the well-known SAC algorithm [22], where the actor network is replaced by a diffusion-modeled action generation module to enhance the actor’s exploration capability. The system framework is described in Fig. 1 and we present the technical details below.

A. The Basics of RL

In the formulated problem, the microgrid community will be operated in a way of sequential decision-making process. The

MDP is represented by a 4-tuple $(\mathcal{S}, \mathcal{A}, \mathcal{P}, \mathcal{R})$, where \mathcal{S} stands for a finite set of observable states of an environment; \mathcal{A} is a finite set of actions; \mathcal{P} is the transition probability function and we have $\sum_{s' \in \mathcal{S}} \mathcal{P}(s_t, a_t, s') = 1$, where s_t is the current state, a_t is the action taken for time t , and s' represents a possible state of s_{t+1} ; \mathcal{R} is the reward function; and γ is the discount factor. A RL agent learns a policy $\pi(a_t|s_t)$ with optimized decision making to maximize the cumulative reward. At each time t , the agent generates and executes action a_t according to the policy π based on state s_t , and receives a reward r_t . The agent keeps observing new states, making actions, and measuring reward, and gradually optimizes the policy π based on continuous interactions with the environment. The details of the tuple are as follows.

1) *State*: The state of the MGC at time t includes crucial microgrid information including load, renewable energy generation, electricity prices, and ESS SoC, constructed as

$$s_t = [P_{LD}(t), P_{RDG}(t), \rho(t), \text{SoC}(t)]. \quad (1)$$

2) *Action*: The power generation or consumption of several major MGC components, including ESS, CDG and load shedding power (LS), is usually controllable. Therefore, they become the focus of the action vector in decision making and control, as

$$a_t = [P_{ESS}(t), P_{CDG}(t), P_{LS}(t)]. \quad (2)$$

3) *Transition Probability*: The transition probability from state s at time $t-1$ to state s' at time t is denoted as $\mathcal{P}_{s \rightarrow s'} = P(s_{t+1}|s_t, a_t)$, given that action a_t is taken at time t . In this paper, we redesign the SAC framework of RL by utilizing the generative capability of diffusion models and developing a diffusion-based action generator based on the latest state. The details will be discussed in the following subsections.

4) *Risk-Aware Reward*: Risk shall be accounted for in many real-world decision-making applications to avoid potentially significant losses or unsafe system behaviors. Often, the importance of a low-risk system even outweighs certain sacrifices of expected returns, as several risk-aware RL algorithms have been proposed in [23], [24]. Specifically for our MGC energy management, risk-awareness is highly important for grid operators to avoid unacceptable spike cost and carbon mission. As such, we incorporate the risk factor into our solution, by optimizing the policy as

$$\pi^* = \arg \max_{\pi} \left\{ \mathbb{E}_{\pi} \left[\sum_{t=1}^{\infty} \gamma r(s_t, a_t) \right] - \lambda_{\text{risk}} R(\pi) \right\}, \quad (3)$$

where we maintain a typical RL reward term with discount factor γ in the first term and further introduce the second term $R(\pi)$ as the risk measurement function associated with policy π . The two terms are balanced by a control parameter λ_{risk} , where a positive value indicates a risk-averse strategy and vice versa. Conditional Value at Risk (CVaR) is commonly used [25], [26] as the risk term $R(\pi)$ to penalize extreme costs, thereby focusing on eliminating the worst-case cost scenarios

$$R(\pi) = \mathbb{E}_{\pi} [\text{Cost} | \text{Cost} > \text{VaR}_{\alpha_{\text{CVaR}}}(\text{Cost})], \quad (4)$$

where α_{CVaR} stands for the percentage of worst-case scenarios to evaluate. For example if $\alpha_{\text{CVaR}} = 0.95$, Eq. (4) measures the 5% CVaR to evaluate the average cost in bad days when the cost is higher than 95% of the others during. Such risk term helps to optimize the worst-case robustness and promote safety and reliability.

B. The Basics of Diffusion Models

The actor network of DIFFCARL is designed based on a diffusion model. Diffusion models are originally designed for image generation. It involves a forward process where noise is gradually added to the data until data becomes Gaussian noise, from which a reverse process starts to generate data that aligns with the distribution of the original data. Inspired by its inherent generative ability in denoising process, we aim to design a diffusion-based optimizer to enhance precision in decision making problems based on environment conditions. The diffusion-based actor network consistently evaluates and optimizes current policy by interacting with the MGC environment. In the reverse process, the diffusion-based actor $\pi_{\theta}(\cdot)$ generates the optimal decision based on conditioning information, which can be viewed as a denoising process starting from Gaussian noise to gradually recover the optimal decision distributions. This design improves the adaptability of DRL and leverages the generative strengths of diffusion models, underscoring their complementary roles in decision-making. Therefore, such combination results in an effective diffusion-based policy optimizer which outperforms conventional DRL approaches in complex and dynamic combinatorial optimization problems [20], [21]. We present technical details of the diffusion model in this part.

1) *Forward Process*: Let \mathbf{x}_0 be the desired action generated by the actor network. \mathbf{x}_0 is a target data sample, which is sampled by a probability distribution of decisions under a condition and the process can be represented as

$$\mathbf{x}_0 = \pi_{\theta}(s) \sim \mathbb{R}^A, \quad (5)$$

where s is the observed state, and θ is the model parameters of the diffusion model. To simply the presentation, we first assume that \mathbf{x}_0 is known. The forward process is performed to add Gaussian noise to the original distribution step by step, deriving a sequence of noised data samples $\mathbf{x}_1, \mathbf{x}_2, \dots, \mathbf{x}_K$, where K is the total diffusion steps. We represent the transition from \mathbf{x}_{k-1} to \mathbf{x}_k as $q(\mathbf{x}_k | \mathbf{x}_{k-1})$, which can be written as

$$q(\mathbf{x}_k | \mathbf{x}_{k-1}) = \mathcal{N}(\mathbf{x}_k | \sqrt{1 - \beta_k} \mathbf{x}_{k-1}, \beta_k \mathbf{I}), \quad (6)$$

where β_k is the forward process variance for $1 \leq k \leq K$, and \mathbf{I} is an identity matrix. We refer to [27] and follow the variational posterior scheduler to schedule β_t at each step as

$$\beta_k = 1 - e^{-\frac{\beta_{\min}}{K} - \frac{2k-1}{2K^2}(\beta_{\max} - \beta_{\min})}, \quad (7)$$

where β_{\min} and β_{\max} are hyper-parameters. The forward process is essentially a Markov process where \mathbf{x}_k is only dependent on \mathbf{x}_{k-1} , and the process creates a mathematical relation between \mathbf{x}_0 and \mathbf{x}_k as

$$\mathbf{x}_k = \sqrt{\bar{\alpha}_k} \mathbf{x}_0 + \sqrt{1 - \bar{\alpha}_k} \boldsymbol{\epsilon}, \quad (8)$$

where we define $\alpha_k = 1 - \beta_k$, $\bar{\alpha}_k = \prod_{i=1}^k \alpha_i$, and $\epsilon \sim \mathcal{N}(0, \mathbf{I})$ as a standard Gaussian noise. The implication is that, with the increase of diffusion step k , \mathbf{x}_k gradually becomes a sample defined by a standard normal distribution at step K .

All above derivations are based on the assumption that \mathbf{x}_0 is known, which, however, may not be feasible for many real-world problems, where the distribution of optimal actions is not fully clear or available. Indeed, the forward process cannot directly obtain the distribution of optimal actions with respect to the observed state. However, it builds up the connection between original and noised data, and the connection is vital for the analysis of the reverse process. For example, we can obtain the reverse conditional probability $q(\mathbf{x}_{k-1}|\mathbf{x}_k, \mathbf{x}_0)$ conditioned on \mathbf{x}_0 as

$$q(\mathbf{x}_{k-1}|\mathbf{x}_k, \mathbf{x}_0) = \mathcal{N}\left(\mathbf{x}_{k-1}; \tilde{\boldsymbol{\mu}}(\mathbf{x}_k, k), \tilde{\beta}_k \mathbf{I}\right), \quad (9)$$

where $\tilde{\boldsymbol{\mu}}(\mathbf{x}_k, k)$ and $\tilde{\beta}_k$ represent the mean and variance of the conditional posterior $q(\mathbf{x}_{k-1}|\mathbf{x}_k, \mathbf{x}_0)$, respectively. They can be calculated from Gaussian conditioning rules as

$$\tilde{\boldsymbol{\mu}}(\mathbf{x}_k, k) = \frac{\sqrt{\bar{\alpha}_k}(1 - \bar{\alpha}_{k-1})}{1 - \bar{\alpha}_k} \mathbf{x}_k + \frac{\sqrt{\bar{\alpha}_{k-1}}\beta_k}{1 - \bar{\alpha}_k} \mathbf{x}_0, \quad (10a)$$

$$\tilde{\beta}_k = \frac{1 - \bar{\alpha}_{k-1}}{1 - \bar{\alpha}_k} \cdot \beta_k. \quad (10b)$$

2) *Reverse Process*: The objective of the reverse process is to denoise a pure noise sample $\mathbf{x}_K \sim \mathcal{N}(0, \mathbf{I})$ to acquire the target sample \mathbf{x}_0 , by removing the noise step by step. Let $p(\mathbf{x}_{k-1}|\mathbf{x}_k)$ be the transition of noise reduction from step k to step $k-1$. As the probability transition function cannot be derived directly, we propose to use a model p_θ to approximate the function, and we have

$$p_\theta(\mathbf{x}_{k-1}|\mathbf{x}_k) = \mathcal{N}(\mathbf{x}_{k-1}; \boldsymbol{\mu}_\theta(\mathbf{x}_k, k, s), \Sigma_\theta(\mathbf{x}_k, k, s)), \quad (11)$$

where s is the observed state. Our target is to train a model p_θ properly, so that the variables in Eq. (10) can be well approximated with $\boldsymbol{\mu}_\theta(\mathbf{x}_k, k, s) \rightarrow \tilde{\boldsymbol{\mu}}(\mathbf{x}_k, k, s)$ and $\Sigma_\theta(\mathbf{x}_k, k, s) \rightarrow \tilde{\beta}_k \mathbf{I}$. Based on Eqs. (7) and (10), $\Sigma_\theta(\mathbf{x}_k, k, s) = \beta_k \mathbf{I}$ is a series of deterministic constant values controlled by variational posterior scheduler. Furthermore, according to Eq. (8), the reconstruction of \mathbf{x}_0 can be obtained by merging multiple Gaussian signals using reparameterization as

$$\mathbf{x}_0 = \frac{1}{\sqrt{\bar{\alpha}_k}} \mathbf{x}_k + \sqrt{\frac{1}{\bar{\alpha}_k} - 1} \cdot \tanh(\boldsymbol{\epsilon}_\theta(\mathbf{x}_k, k, s)), \quad (12)$$

where $\boldsymbol{\epsilon}_\theta(\mathbf{x}_k, k, s)$ is a multi-layer neural network model parameterized by $\boldsymbol{\theta}$ which approximates the noises conditioned on state s to be denoised. We use the derived \mathbf{x}_0 to calculate Eq. (10) and we can estimate the mean $\tilde{\boldsymbol{\mu}}(\mathbf{x}_k, k, s)$ by

$$\tilde{\boldsymbol{\mu}}(\mathbf{x}_k, k, s) = \frac{1}{\sqrt{\bar{\alpha}_k}} \left(\mathbf{x}_k - \frac{\beta_k \cdot \tanh \boldsymbol{\epsilon}_\theta(\mathbf{x}_k, k, s)}{\sqrt{1 - \bar{\alpha}_k}} \right). \quad (13)$$

Based on the noise approximation model $\boldsymbol{\epsilon}_\theta(\mathbf{x}_k, k, s)$, we sample \mathbf{x}_{k-1} from Eqs. (11) and (13). The properties of a Markov process allows us to derive the generation distribution $p_\theta(\mathbf{x}_0)$ as

$$p_\theta(\mathbf{x}_0) = p(\mathbf{x}_K) \prod_{k=1}^K p_\theta(\mathbf{x}_{k-1}|\mathbf{x}_k), \quad (14)$$

where $p(\mathbf{x}_K)$ is a standard Gaussian distribution as the start of the reverse process. Furthermore, we reparameterize the noise term instead to predict \mathbf{x}_{k-1} as

$$\mathbf{x}_{k-1} = \mathcal{N}(\mathbf{x}_{k-1}; \boldsymbol{\mu}_\theta(\mathbf{x}_k, k, s), \Sigma_\theta(\mathbf{x}_k, k, s)). \quad (15)$$

C. DIFFCARL Algorithm Description

DIFFCARL is RL-based and the training process begins with the RL agent observing the environment to obtain initial state s_0 . The agent will utilize the diffusion model to iteratively perform denoising and generate an action based on the current state. Specifically at each step t , the actor generates a probability distribution $\pi_\theta(s_t)$ over all possible actions based on the observation s_t . Then, an action $a_t \sim \pi_\theta(s_t)$ is sampled and fed into the environment. The environment processes the action and sends back a new state s_{t+1} and a reward r_t as the feedback to the agent. The agent records the transitions by interacting with the environment and the transitions from different time steps are saved into the replay buffer \mathcal{B} .

1) *Action Entropy Regularized Policy Improvement*: One of key objectives of RL is to improve the actor network, or policy, so that optimal actions can be generated based on the observed states. Typically, the policy is gradually optimized by sampling batches of transitions from replay buffer \mathcal{B} and maximizing the expectation of Q values over all actions as

$$\max_{\boldsymbol{\theta}} \pi_\theta^T(s) Q_\phi^{\text{risk}}(s) + \alpha_{\text{ent}} H(\pi_\theta(s)), \quad (16)$$

where the first term, $\pi_\theta^T(s)$ denotes current policy and $Q_\phi^{\text{risk}}(s)$ is a risk-adjusted Q-value function which outputs a Q-value q . The second term models the entropy of the action probability $\pi_\theta(s)$, and can be calculated as $H(\pi_\theta(s)) = -\pi_\theta^T(s) \log \pi_\theta(s)$. α_{ent} is the temperature co-efficiency for controlling the strength of the entropy to encourage exploration.

By maximizing Eq. (16), the agent optimizes the actor network in a direction of selecting the actions with high Q-values. The parameters of the network are updated based on the gradient descent as

$$\boldsymbol{\theta}_{e+1} \leftarrow \boldsymbol{\theta}_e - \eta_a \cdot \mathbb{E}_{(s,a,s',r) \sim \mathcal{B}} \left(\nabla_{\boldsymbol{\theta}_e} \left[-\alpha_{\text{ent}} H(\pi_\theta(s)) - \pi_\theta^T(s) Q_\phi^{\text{risk}}(s) \right] \right), \quad (17)$$

where η_a represents the learning rate of the actor network and e identifies an epoch.

2) *Risk-sensitive Q-function Improvement*: Q-function network $Q_\phi(s)$ as the critic is crucial for DIFFCARL for evaluating policy $\pi_\theta(s)$ and we design the risk-adjusted Q-function $Q_\phi^{\text{risk}}(s)$ based on CVaR. In every epoch e , we update the Q-function effectively and utilize the temporal difference error to minimize the loss function

$$\mathcal{L}_Q^{\text{risk}}(\phi_e) = \mathbb{E}_{(s,a,s',r) \sim \mathcal{B}} \left[\left(Q_\phi^{\text{risk}}(s, a) - y_{\text{CVaR}} \right)^2 \right], \quad (18)$$

where $Q_\phi^{\text{risk}}(s, a)$ represents the risk-sensitive Q-value given by the critic networks corresponding to the state and action at each epoch e , and the CVaR-based target y_{CVaR} is updated by

$$y_{\text{CVaR}} = r + \gamma \cdot \text{CVaR}_{\alpha_{\text{CVaR}}} \left(\min_{i=1,2} \hat{Q}_{\hat{\phi}_e^i}(s', a') - \alpha_{\text{ent}} \log \hat{\pi}_{\theta_e}(s') \right), \quad (19)$$

where r stands for the immediate reward, γ denotes the discount factor, $i = 1, 2$ represent the different critic networks, $\text{CVaR}_{\alpha_{\text{CVaR}}}(\cdot)$ is a CVaR-regulated term based on Eq. (4), $\alpha_{\text{ent}} \log \hat{\pi}$ is an action entropy term, while $\hat{\pi}$ and \hat{Q} stand for the target actor and critic networks with parameters $\hat{\theta}$ and $\hat{\phi}$, respectively.

3) *Soft-Update*: In DIFFCARL, we adopt soft-update for the actor and critic networks to improve convergence stability during training. Instead of updating network parameters abruptly as hard-update does, parameters are updated mildly and such a smooth transition helps prevent large swings or oscillations in estimations and reduce the risk of divergence. In practice, a hyper-parameter $\tau \in (0, 1]$ is used to control the update rate, and we have

$$\hat{\theta}_{e+1} \leftarrow \tau \theta_e + (1 - \tau) \hat{\theta}_e, \quad (20a)$$

$$\hat{\phi}_{e+1} \leftarrow \tau \phi_e + (1 - \tau) \hat{\phi}_e, \quad (20b)$$

where $\hat{\theta}$ and $\hat{\phi}$ are updated through soft-update instead of being updated directly based on gradient descent. Overall, DIFFCARL iteratively updates both actor and critic networks epoch by epoch until reaching convergence. We present the pseudo-code of DIFFCARL in Algorithm 1. The computational complexity of the proposed DIFFCARL is $\mathcal{O}(E[C(V + KN_{\theta}) + (d + 1)(N_{\theta} + N_{\phi}) + d \log d])$, where E stands for training episodes, C is the transitions collected per episode, V represents the complexity of the environment, K is the denoising steps, N_{θ} and N_{ϕ} are the parameter numbers of the actor and critic networks respectively, and d stands for the batch size. The space complexity of DIFFCARL is $\mathcal{O}(2N_{\theta} + 4N_{\phi} + B(2|\mathcal{S}| + |\mathcal{A}| + 1))$, where B represents the capacity of the replay buffer \mathcal{B} , while $|\mathcal{S}|$ and $|\mathcal{A}|$ are the dimensions of states and actions respectively.

III. RESULTS AND DISCUSSIONS

In this section, we analyze DIFFCARL and demonstrate its outstanding performance by comparing to other existing methods. Besides, we provide insights into the use of DIFFCARL and its advantages in MGC energy management.

A. Experimental Setup

We present the experimental setup in the following aspects.

1) *Computing Setup*: Our experiments were conducted by a workstation with an NVIDIA GeForce RTX 4090 GPU with 24GB memory and an Intel Core Ultra 7 265KF 20-Core CPU and 64GB of DDR5 RAM. The operating system is Ubuntu 24.04.2 LTS with CUDA V12.2 toolkit. Besides, our experiments are organized with the following details.

2) *Dataset*: To evaluate our proposed method's performance, we conducted experiments on multiple datasets, including real-world data and synthetic data. For real-world data we choose the PJM dataset contains publicly available energy system data provided by Pennsylvania-Jersey-Maryland

Algorithm 1: DIFFCARL: Diffusion-Modeled Carbon and Risk-Aware Reinforcement Learning

Input: A well-defined MGC environment \mathcal{E} , number of maximum training episodes E , Transitions per training step C , weight of soft update τ , discount factor γ , temperature co-efficiency α , learning rate of actor network η_a , learning rate of critic networks η_c , confidence level of CVaR α_{CVaR} , batch size d

Output: A DIFFCARL policy π^* with parameters θ^*

- 1 Initialize a diffusion policy π_{θ} with parameters θ , Q-function networks Q_{ϕ} with parameters ϕ and a replay buffer \mathcal{B} ;
- 2 Initialize target network parameters $\hat{\theta} \leftarrow \theta$, $\hat{\phi} \leftarrow \phi$;
- 3 **for** training episode $e \leftarrow 1$ **to** E **do**
- 4 **for** transition updates $c \leftarrow 1$ **to** C **do**
- 5 Initialize a normal distribution $x_K \sim \mathcal{N}(\mathbf{0}, \mathbf{I})$;
- 6 Observe state s ;
- 7 **for** denoising step $k \leftarrow K$ **to** 1 **do**
- 8 Scale a denoising factor $\epsilon(x_k, k, s)$ based on x_k ;
- 9 Calculate the distribution \mathbf{x}_{k-1} based on (11), (13), (15).
- 10 **end**
- 11 Calculate probability distribution $\pi_{\theta}(s)$ of \mathbf{x}_0 based on a softmax function;
- 12 Select an optimal action a based on $\pi_{\theta}(s)$;
- 13 Execute a and observe the environment feedback with reward r and next state s' ;
- 14 Save the transition (s, a, s', r) in the replay buffer \mathcal{B} ;
- 15 **end**
- 16 Sample a transition batch data $\mathcal{D} = \{(s, a, s', r)\}_d$ from replay buffer \mathcal{B} ;
- 17 Estimate the α_{CVaR} -quantile of the target return distribution for each (s, a) in the batch \mathcal{D} by (4);
- 18 Update the policy parameters θ based on \mathcal{D} by (17);
- 19 Update the Q-function network parameters ϕ by minimizing (18);
- 20 Update parameters of target networks $\hat{\theta}$ and $\hat{\phi}$ by (20);
- 21 **end**
- 22 **return** A DIFFCARL policy π^* with parameters θ^*

(PJM) Interconnection, one of the largest regional transmission organizations. The PJM dataset contains high temporal resolutions and various market features, and has been widely used by many research studies [12], [28]. We adopt following data profiles for our designed MGC environment: 1) solar (PV) generation; 2) wind turbine (WT) generation; 3) load; and 4) real-time energy market locational marginal pricing (LMP). The PJM dataset provides hourly measurements over one year. We first apply preprocessing to eliminate random noise and outlier spikes. To avoid the disturbance of seasonal weather variations, the preprocessed data is sorted monthly, with the first three weeks allocated to the training set and the fourth week reserved for testing. The synthetic dataset is generated based on a nominal data profile, with 20% white noise added to the real data to introduce variability across samples. Compared to the real-world dataset, the synthetic data spans a narrower value range but exhibits greater randomness in temporal continuity.

3) *Microgrid Setup*: We design DIFFCARL to be versatile for various MGC settings. Here, we follow the common settings based on existing studies to demonstrate the effectiveness of DIFFCARL. The details of the MGC environment parameters can be found in Table I.

TABLE I: The settings of the MGC environment parameters used in the experimental study.

Parameters	Description	Values
E_{ESS}	ESS Capacity (kWh)	200
$[\eta_{\text{ch}}, \eta_{\text{dis}}]$	ESS Charging and Discharging Coefficiency	[0.9, 0.95]
$[P_{\text{ch}}^{\text{max}}, P_{\text{dis}}^{\text{max}}]$	ESS Charging and Discharging Power Limit (kW)	[200, 200]
$[\gamma_{\text{ch}}, \gamma_{\text{dis}}]$	ESS Charging and Discharging Cost Factor (S\$/kWh)	[0.005, 0.005]
$[E_{\text{ESS}}^{\text{min}}, E_{\text{ESS}}^{\text{max}}]$	ESS Storage Limit (kWh)	[200, 1,800]
$E_{\text{ESS}}(0)$	ESS Initial Storage (kWh)	1000
$[a, b, c]$	CDG Cost Coefficient	[0.004, 0.066, 0.7]
$[P_{\text{CDG}}^{\text{min}}, P_{\text{CDG}}^{\text{max}}]$	CDG Power Limit (kW)	[0, 200]
$R_{\text{CDG}}^{\text{max}}$	CDG Power Maximum Ramp Rate (kW/h)	20
α_{LD}	Maximum Load Shedding Rate	0.5
λ_{LD}	Load Shedding Penalty (S\$/kWh)	1
ρ_{Carbon}	Carbon Price (S\$/kg CO2)	0.025
$[\omega_{\text{CDG}}, \omega_{\text{Grid}}]$	Carbon Density (kg CO2/kWh)	[0.9, 0.412]

TABLE II: The structure of actor and critic networks in DIFFCARL.

Networks	Layers	Activation	Neurons
Actor	SinusoidalPosEmb	-	16
	fc	mish	32
	fc	mish	16
	concat	-	-
	fc	mish	128
	fc	mish	128
	fc	tanh	45
Critic	fc	mish	128
	fc	mish	128
	fc	-	45

4) *DIFFCARL Model Design*: DIFFCARL follows a soft-actor critics (SAC) framework for MGC energy scheduling with the key novelty of upgrading the actor network with diffusion modelling. We describe the network structure in Table II and list the settings of hyper-parameters in Table III.

Specifically for the actor and double critic networks, we follow a similar network configuration to mitigate overestimation [22]. The structures of the actor and critic networks are described in Table II. In the actor network, we use sinusoidal position embedding layer `SinusoidalPosEmb` to process temporal information in diffusion to derive time embedding vectors. `concat` allows concatenation of sinusoidal embeddings, denoising step k and state s . Besides, the parameters of the networks are optimized by `adam` optimizer and the training related hyper-parameters are available in Table III.

B. Case Study

We first present a case study to illustrate and validate a one-day energy scheduling produced by DIFFCARL. The results are shown in Fig. 2, and we have the following observations.

First, DIFFCARL can maintain supply-demand balance as shown in Fig. 2a. In the figure, the positive stacked bars

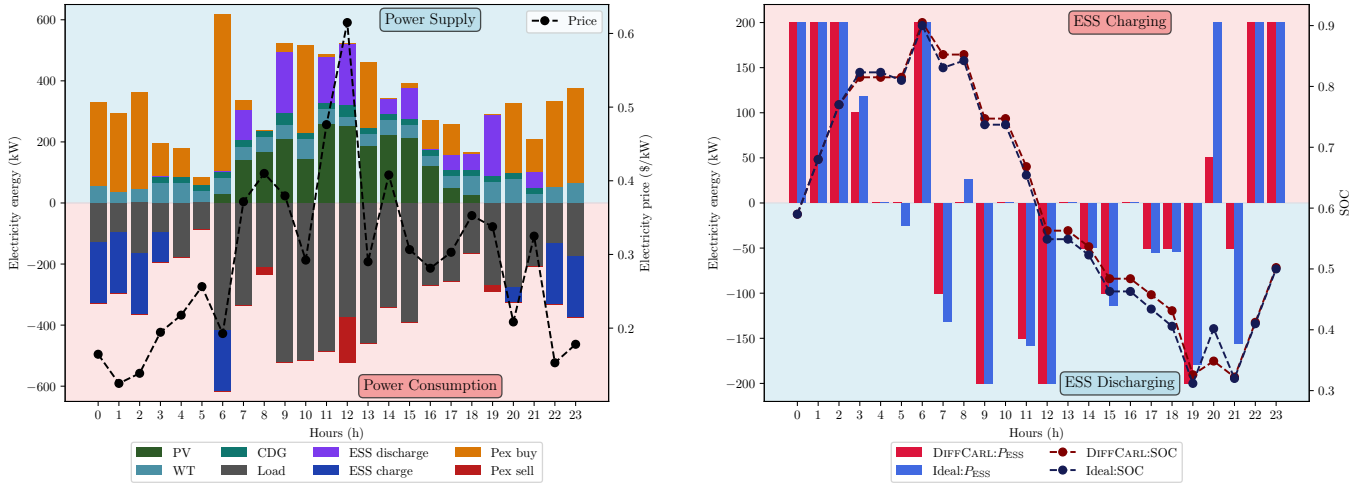
TABLE III: The settings of DIFFCARL hyper-parameters.

Parameters	Description	Values
η_a	Learning rate of the actor	1×10^{-4}
η_c	Learning rate of the critics	1×10^{-3}
τ	Weight of soft update	5×10^{-3}
λ_{wd}	Weight decay	1×10^{-4}
α_{ent}	Action entropy regularization temperature	0.05
λ_{risk}	Risk sensitivity coefficient	0.1
α_{CVaR}	Confidence level for computing CVaR	0.95
γ	Discount factor	0.95
K	Denoising steps in diffusion model	10
d	Batch size	256
B	Capacity of replay buffer	1×10^6
E	Maximum training episodes	2000
C	Transitions per training step	1000

correspond to energy supply, contributed by renewable, CDG, ESS (discharge), and utility grid (purchase). The negative bars represent energy demand, for load, ESS charging, and selling electricity to the grid. In each hour, DIFFCARL balances the supply and demand energy while optimizing operational cost and carbon emission. Second, DIFFCARL maximizes the utilization of renewable. During periods with high renewable output and low demand, purchases from the utility grid is minimized, or MGC can even sell electricity to the grid. Similarly, DIFFCARL tends to purchase more energy when necessary, e.g., with reduced renewable.

The usage of CDG is minimal and adaptive throughout the day. This suggests that CDG is a cost- and carbon-sensitive energy dispatch unit. CDG is activated often when the renewable and ESS are insufficient to well cover the demand. Besides, CDG has lower ramp rate than ESS and the priority of activating it can be lower under urgent energy usage scenarios. ESS serves a similar role as CDG but owns its unique characteristics, e.g., large maximum ramp rate and non-carbon-intensive. Seen from Figure 2, ESS is being charged during off-peak hours with low electricity prices. Similarly, discharge happens more often during peak hours with high prices. Overall, this case study demonstrates clearly that DIFFCARL is able to produce a valid and effective schedule in operating the MGC system.

DIFFCARL deals with uncertain future system dynamics. We would like to further compare its performance with the best possible scheduling. Here, we introduce OFFLINE, which assumes full knowledge of future events and performs offline optimal decision-making to provide the theoretical upper bound of the optimization performance. Note that OFFLINE's assumption is unrealistic as the future dynamics of the system is unknown or uncertain and the decision-making cannot be in an offline manner. In Fig. 2b, ESS output and its SoC profiles are compared between DIFFCARL and OFFLINE. Both strategies exhibit a clear pattern of charging at night and early hours with low prices or demand, and discharging during daytime and peak hours. DIFFCARL achieves very similar charging/discharging profiles compared to OFFLINE. Besides, we notice that DIFFCARL is not aggressive in ESS operations, for its awareness of risks and potential penalties on violating



(a) Electrical power balance and electricity price under DIFFCARL. (b) ESS operation and SoC variation under DIFFCARL and OFFLINE.

Fig. 2: Case study results over a 24-hour test day. (a) shows the electrical power balance including contributions from photovoltaic (PV), wind turbine (WT), community diesel generator (CDG), energy storage system (ESS), and grid interactions (Pex buy/sell), along with the dynamic electricity price under the proposed DIFFCARL policy. (b) shows the corresponding ESS operations, including charging and discharging behaviors, and the resulting state-of-charge (SoC) trajectory, compared against an ideal but unrealistic benchmark method OFFLINE.

the SoC constraints.

C. Comparison Study

We compare DIFFCARL with several comparison algorithms to demonstrate its effectiveness in energy scheduling.

1) *Comparison Algorithms*: We consider a few benchmark algorithms as the baselines, including DQN, DDPG and SAC where technical details can be found in literature. We also implement several methods including OFFLINE described above and the others detailed below.

DAY-AHEAD: This algorithm does not make unrealistic assumptions as OFFLINE. It makes predictions of the next-day system dynamics and aims to make the best decisions based on the predictions, which, are not the ground-truth.

MYOPIC: This method is based on greedy algorithm and decisions are made step-by-step. In each step, the method collects available information of the step and optimizes the decision-making of the step without considering future consequences.

MPC: This method addresses the limitations of the above algorithms by incorporating both future predictions and real-time feedback into its decision-making. Predictions are assumed to be more accurate for near-future and less accurate for long-future.

2) *Operating Cost*: We define a relative cost metric to compare the performance of a given algorithm against DIFFCARL as

$$\frac{C_{\text{DIFFCARL}} - C_{\text{COMP}}}{C_{\text{DIFFCARL}}} \times 100\%, \quad (21)$$

where C_{COMP} and C_{DIFFCARL} are the costs of the comparison algorithm and DIFFCARL, respectively. The improvement is represented as a percentage and a negative value means that DIFFCARL is better than the comparison algorithm, and vice versa. The comparison results are shown in Table IV.

First, let us consider an MGC scenario with 2 microgrids, represented as 2MG in the table. It consists of 2 loads, 2

PVs, 2 WTs, 2 CDGs and 2 ESS units. Compared to all the tested online algorithms, DIFFCARL achieves the lowest cost and carbon emission. Overall, DIFFCARL's cost performance is significantly better than other baselines, and DIFFCARL outperforms DAY-AHEAD the most with 30.1% improvement. We further compare DIFFCARL with the unrealistic OFFLINE with perfect and optimal energy scheduling. The results show that DIFFCARL can approximate the optimal performance by 98.2%, which aligns with our observation in the case study that DIFFCARL develops a near-optimal policy. A reason for DIFFCARL's competitive performance is that the diffusion model in the actor network is effective in approximating the potentially complex distribution of the optimal actions.

Among the comparison algorithms, DAY-AHEAD, MYOPIC, and MPC are not learning-based and their performance is relatively not competitive. DAY-AHEAD is basically a static algorithm and performs poorly due to its lack of adaptability. MYOPIC and MPC are considered as online methods which perform scheduling based on real-time information. Their performance is constrained by the prediction accuracy and scheduling horizon. As a result, they are only capable to deal with scenarios that are similar to the nominal data profile, e.g., with less challenging and more accurate predictions, and the performance with real-world dataset suffers. MYOPIC and MPC both lack temporal generalization or adaptability to uncertainty and variability compared to diffusion-based DIFFCARL, and the performance gaps are 17.6% and 8.0%, respectively.

RL-based algorithms have been the state-of-the-art for energy scheduling, and they outperform the non-RL algorithms presented above. Our proposed DIFFCARL manages to produce improved scheduling compared to these competitive algorithms, including DQN, SAC and DDPG. Among these algorithms, DQN performs the worst with a 6.4% gap. DQN is a conventional method and it emulates table-seeking Q-

TABLE IV: Performance comparisons between DIFFCARL and different benchmarks. Negative percentages mean the comparison algorithms are outperformed by DIFFCARL. DIFFCARL can well approximate the optimal performance by OFFLINE. Compared to the rest of other algorithms, it achieves the best performance for all scenarios including 2MG, IEEE 15-bus and 33-bus in terms of both overall cost and carbon emission.

Algorithms	2MG Case			IEEE 15-bus			IEEE 33-bus		
	Cost	Carbon	Improv.	Cost	Carbon	Improv.	Cost	Carbon	Improv.
DAY-AHEAD	965.30	92.24	-30.12%	3,273.77	198.19	-26.67%	9,267.06	686.81	-26.79%
MYOPIC	872.35	88.07	-17.59%	3,084.49	197.31	-19.35%	8,916.11	642.75	-21.99%
MPC-8	801.36	67.77	-8.02%	2,891.45	171.07	-11.88%	8,521.62	581.18	-16.59%
DQN	789.21	64.72	-6.38%	2,835.14	160.62	-9.70%	8,351.87	553.97	-14.27%
SAC	762.14	63.52	-2.73%	2,701.24	154.41	-4.52%	8,065.71	532.94	-10.36%
DDPG	758.80	61.21	-2.28%	2,609.01	148.26	-0.95%	7,551.94	498.84	-3.32%
DIFFCARL (ours)	741.86	59.25	—	2,584.46	144.75	—	7,308.61	483.95	—
OFFLINE	724.84	54.84	2.29%	2,461.49	131.55	4.76%	7,064.51	457.38	3.34%

learning algorithm which is poorly suited for fine-grained problems like MGC energy scheduling. SAC and DDPG perform better, but still worse than DIFFCARL with 2.7% and 2.3% higher costs, respectively. RL-based methods are more adaptive to unprecedented scenarios and data variance due to its learning based pattern by actively interacting with the MGC environment. DIFFCARL, as an enhanced RL, not only inherits the RL advantages, but also captures temporal awareness with its generative mechanism based on diffusion modelling.

We further investigate the algorithms' performance under two standard IEEE test feeders, including IEEE 15-bus and 33-bus systems. The former has 10 loads, 2 PVs, 3 ESS units, and 2 CDGs, and the latter consists of 26 loads, 5 PVs, 7 ESS units, and 5 CDGs. The results are summarized in Table IV. The results demonstrate that DIFFCARL's competitiveness is not limited to the 2MG case and the algorithm can outperform comparison algorithms consistently across different power system scales, e.g., under IEEE 15-bus and 33-bus systems. Compared to traditional scheduling strategies including DAY-AHEAD, MYOPIC, and MPC, DIFFCARL achieves substantial reductions in both operational cost and carbon emissions, with cost savings exceeding 15%. While RL-based methods such as DQN, SAC and DDPG show improved efficiency compared to numerical methods, DIFFCARL still surpasses them in IEEE 33-bus system by 14.3%, 10.4% and 3.3%, respectively.

In summary, the results show that DIFFCARL remains robust as system complexity increases, indicating strong scalability and generalization capability. The results validate DIFFCARL as a highly effective and sustainable framework for intelligent energy management in MGC systems.

3) *Learning and Convergence*: DIFFCARL, together with DQN, SAC, and DDPG, are RL-based and learn optimal policies by maximizing the reward during training. We visualize learning curves of these algorithms in Fig. 3 with 250k steps. Seen from the figure, DIFFCARL converges to the largest reward at the end of training. During training process, DIFFCARL's best test reward is -666.5 which is higher than DQN, SAC and DDPG. Among all benchmarks, DIFFCARL brings the best performance overall, consistently yielding the highest test reward throughout training. Meanwhile, its fast convergence allow the agent to swiftly get a well-trained policy even before 50k steps. Lastly, the smooth curve with minimal

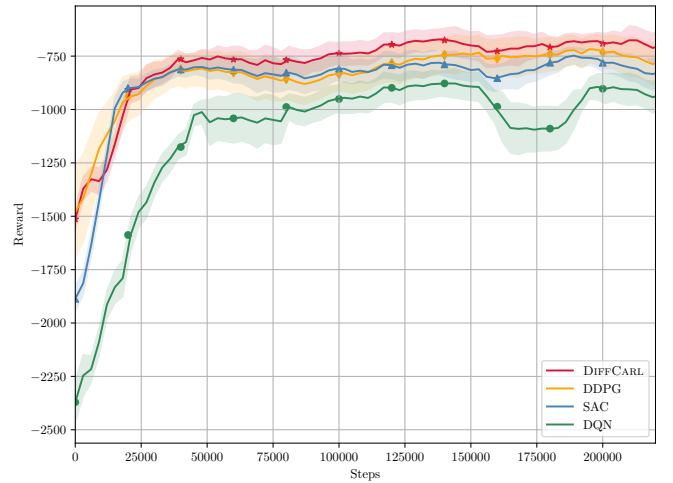


Fig. 3: A comparison of learning curves under different RL policies. DIFFCARL converges fast and stably outperforms other RL policies with higher test reward.

fluctuations indicates a very robust and stable learning process of DIFFCARL.

DIFFCARL is able to achieve higher rewards during most of the training process, indicating that its policy outperforms the policies of the other RL-based methods. One of the most inspiring features of the diffusion modeled RL is that a noise predictor is applied to generate actions, which significantly helps to develop a satisfactory policy even in unprecedented scenarios, eliminating the randomness in action generation and reducing high-cost operations in scheduling.

D. DIFFCARL Carbon- and Risk-awareness

DIFFCARL not only minimizes the total cost with optimized energy scheduling, but also achieves carbon- and risk-awareness. In this part, we specifically present the results of DIFFCARL's carbon emission and risk-aware scheduling.

1) *Carbon Emission*: Carbon emission is part of the formulated problem in this study. As such, the comparison algorithms incorporating the same cost functions are essentially carbon-aware, same as DIFFCARL. Here, we present DIFFCARL's carbon emission compared to the rest RL-based

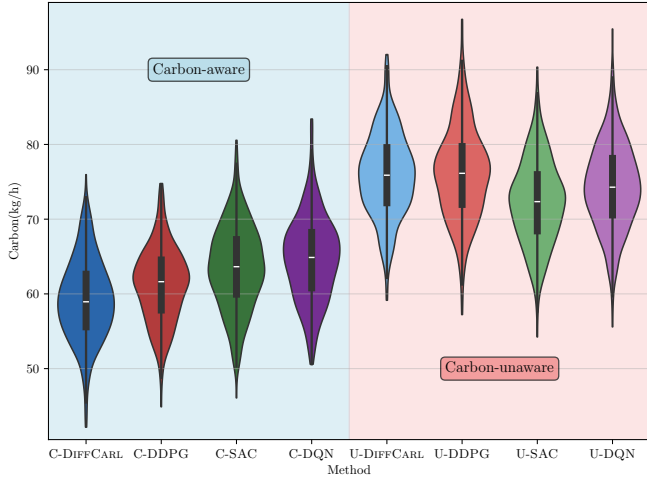


Fig. 4: Carbon emission distributions under carbon-aware (C-) and carbon-unaware (U-) policies. Carbon-aware (C-) methods show lower carbon emission with less variance than their carbon-unaware (U-) alternatives. DIFFCARL shows the lowest carbon emission among carbon-aware (C-) policies.

algorithms that are carbon-aware. We further demonstrate the impact of removing carbon factors from the problem formulation and present the results of non-carbon-aware algorithms. Fig. 4 shows the carbon emission of different tested algorithms and some numerical results are available in Table IV.

First, carbon shall be reflected in energy scheduling problems. Among all RL policies, the carbon-aware group methods have consistently lower carbon emissions than their carbon-unaware counterparts. Carbon-unaware methods show wider and higher distribution tails, especially U-DDPG and U-DQN, suggesting greater variability and higher average emissions. Compared with U-DIFFCARL’s carbon emission 64.7 kg/h, C-DIFFCARL has much less emission with 59.3 kg/h, which indicates approximately 28.7% less carbon, significantly promoting a greener operation of microgrids. Meanwhile, it is obvious that all listed carbon-aware methods allow the MGC to produce much less carbon than their carbon-unaware alternatives. This indicates how algorithms’ carbon-awareness reduces environmental impact during MGC operations and thereby contributing to sustainable development.

Among the carbon-aware RL algorithms, C-DIFFCARL outperforms the rest regarding carbon emission. Our algorithm has the lowest median carbon emission 58.9 kg/h with a narrow distribution, demonstrating its reliability in minimizing carbon emission. In conclusion, the results highlight the importance of carbon-awareness for minimizing carbon emission overtime, and the carbon-aware DIFFCARL is the most robust and effective among the tested algorithms.

2) *Risk Sensitivity*: DIFFCARL is risk-aware and we discuss the relationship between cost and risk in this part. We applied CVaR to eliminate worst case outcomes with a high risk of introducing high operational costs. DIFFCARL’s sensitivity on risks can be controlled by a risk parameter λ based on Eq. (3), where a positive λ indicates a risk-averse strategy while a negative value implies risk-seeking. Here, we consider three

levels of risk sensitivities, including risk-averse, risk-neutral, and risk-seeking [25]. The results are shown in Fig. 5 and the discussions are as below.

The results reveal clear trade-offs between cost optimization and risk management in DIFFCARL policies. Seen from the figure, risk-seeking leads to the most significant cost fluctuations, e.g., with a long distribution. This implies that the pursuit of high-risk cost minimization comes with the increase of system instability and variability. Meanwhile, risk-averse policies provide more predictable costs at a moderate premium. It suggests that moderate risk-seeking behavior does not influence cost efficiency much, but significantly increase the system stability.

When examining median costs across different risk sensitivity levels, the risk-neutral emerges as the top performer with cost S\$751.8, followed by risk-seeking policy with $\lambda = -0.1$ with nearly the same cost, S\$752.0. Risk-averse policies command slightly higher costs. When $\lambda = 0.1$, the cost is S\$761.7, and the gap between risk-neutral and risk-averse is about S\$10. When $\lambda = 1$, the gap increases significantly to S\$33. A very aggressive risk-seeking policy with $\lambda = -1$ performs poorly with the highest median cost S\$789.0, suggesting that extreme risk-seeking behavior is counterproductive and unstable and DIFFCARL’s risk-awareness is necessary.

Risk-averse policies demonstrate their primary value proposition through significantly reduced volatility. The risk-averse policy of $\lambda = 1$ achieves the most stable performance with a standard deviation of only S\$84.1, representing a 21% reduction compared to the neutral policy’s S\$106.4. While a moderate policy with $\lambda = 0.1$ provides moderate stability improvement with a standard deviation of S\$97.0, offering a 9% volatility reduction. These policies also provide better worst-case protection, with maximum costs ranging from S\$1,024 to S\$1,062 compared to S\$1,096 for risk-neutral. Risk-seeking policies present a more uncertain and instable feature. Both risk-seeking variants show approximately 18% higher volatility than risk-neutral, and their worst case costs range from S\$1,180 to S\$1,316, which brings up extra concern in real-world energy applications.

Overall, experiments demonstrate that risk-averse policy with $\lambda = 0.1$ emerges as the optimal policy for most applications, successfully balancing cost efficiency with manageable risk exposure. For risk-constrained environments, a more conservative policy of $\lambda = 1$ provides excellent volatility reduction at a reasonable cost premium, making it ideal for applications requiring predictable and acceptable budgets. The results reveal that moderate risk preferences tend to outperform extreme positions by striking a balance in eliminating uncertainty and optimizing cost, which maximizes the effectiveness of DIFFCARL policies. In reality, the users may choose and adopt their own risk sensitive policy according to their needs, with a customized emphasis on safety or performance.

IV. CONCLUSION

In this paper, we have proposed DIFFCARL, a diffusion-modeled carbon- and risk-aware reinforcement learning algorithm for microgrid energy scheduling and optimization.

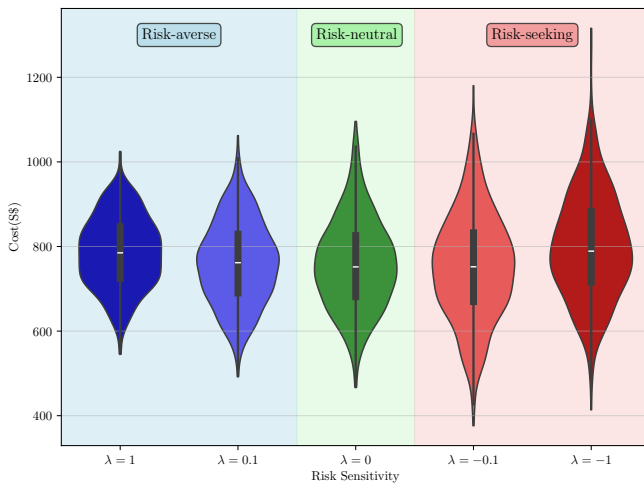


Fig. 5: Cost distributions under DIFFCARL policies with varying risk-sensitivity parameters. $\lambda > 0$ indicates risk-averse behavior with tighter cost distributions, while $\lambda < 0$ indicates risk-seeking behavior with broader cost distributions.

DIFFCARL enables grid operators to schedule microgrids effectively while promoting sustainability and robustness. Integrating a diffusion-based policy framework with explicit carbon- and risk-sensitive objectives balances operational efficiency with environmental and reliability constraints. Extensive experiments have demonstrated that DIFFCARL achieves 2.3–30.1% lower operational costs than baseline methods, reduces carbon emissions by 28.7% compared to its carbon-unaware variant, and shows lower performance variability under dynamic and uncertain conditions. These results have underscored the potential of GenAI-based models in advancing intelligent and sustainable energy systems. In the future, we would like to investigate the applicability of DIFFCARL to different microgrid configurations and settings. We also plan to explore DIFFCARL’s adaptation to related domains such as battery energy storage management and smart manufacturing, where uncertainty, sustainability, and dynamic scheduling are also critical.

REFERENCES

- [1] N. Zhi, X. Xiao, P. Tian, and H. Zhang, “Research and prospect of multi-microgrid control strategies,” *Electric Power Automation Equipment*, vol. 36, pp. 107–115, 04 2016.
- [2] Z. Li and Y. Xu, “Optimal coordinated energy dispatch of a multi-energy microgrid in grid-connected and islanded modes,” *Applied Energy*, vol. 210, pp. 974–986, 2018. [Online]. Available: <https://www.sciencedirect.com/science/article/pii/S0306261917312230>
- [3] M. Alipour, K. Zare, and M. Abapour, “Minlp probabilistic scheduling model for demand response programs integrated energy hubs,” *IEEE Transactions on Industrial Informatics*, vol. 14, no. 1, pp. 79–88, 2017.
- [4] M. Hosseinzadeh and F. R. Salmasi, “Robust optimal power management system for a hybrid ac/dc micro-grid,” *IEEE Transactions on Sustainable Energy*, vol. 6, no. 3, pp. 675–687, 2015.
- [5] D. Thomas, O. Deblecker, and C. S. Ioakimidis, “Optimal operation of an energy management system for a grid-connected smart building considering photovoltaics’ uncertainty and stochastic electric vehicles’ driving schedule,” *Applied Energy*, vol. 210, pp. 1188–1206, 2018.
- [6] A. Parisio, E. Rikos, and L. Glielmo, “A model predictive control approach to microgrid operation optimization,” *IEEE Transactions on Control Systems Technology*, vol. 22, no. 5, pp. 1813–1827, 2014.
- [7] M. Petrollese, L. Valverde, D. Cocco, G. Cau, and J. Guerra, “Real-time integration of optimal generation scheduling with mpc for the energy management of a renewable hydrogen-based microgrid,” *Applied Energy*, vol. 166, pp. 96–106, 2016.
- [8] P. Tian, X. Xiao, K. Wang, and R. Ding, “A hierarchical energy management system based on hierarchical optimization for microgrid community economic operation,” *IEEE Transactions on Smart Grid*, vol. 7, no. 5, pp. 2230–2241, 2015.
- [9] Y. Liu, S. Gao, C. Xiang, M. Yu, and K. T. Tan, “Distributed optimal energy management of a microgrid community,” in *2022 IEEE 17th International Conference on Control & Automation (ICCA)*. IEEE, 2022, pp. 832–837.
- [10] V.-H. Bui, A. Hussain, and H.-M. Kim, “Double deep q -learning-based distributed operation of battery energy storage system considering uncertainties,” *IEEE Transactions on Smart Grid*, vol. 11, no. 1, pp. 457–469, 2019.
- [11] A. A. Amer, K. Shaban, and A. M. Massoud, “Drl-hems: Deep reinforcement learning agent for demand response in home energy management systems considering customers and operators perspectives,” *IEEE Transactions on Smart Grid*, vol. 14, no. 1, pp. 239–250, 2022.
- [12] S. Gao, C. Xiang, M. Yu, K. T. Tan, and T. H. Lee, “Online optimal power scheduling of a microgrid via imitation learning,” *IEEE Transactions on Smart Grid*, vol. 13, no. 2, pp. 861–876, 2021.
- [13] Y. Zhao, S. Gao, J. Wang, C. Li, M. Yu, and C. Xiang, “Online cooperative optimal power scheduling of multiple microgrids via hierarchical imitation learning,” in *2024 IEEE 18th International Conference on Control & Automation (ICCA)*. IEEE, 2024, pp. 30–35.
- [14] S. Gao, Y. Xu, Z. Zhang, Z. Wang, X. Zhou, and J. Wang, “Multi-agent imitation learning based energy management of a microgrid with hybrid energy storage and real-time pricing,” *IEEE Internet of Things Journal*, 2025.
- [15] I. Kostrikov, O. Nachum, and J. Tompson, “Imitation learning via off-policy distribution matching,” *arXiv preprint arXiv:1912.05032*, 2019.
- [16] A. Dolatabadi, H. Abdeltawab, and Y. A.-R. I. Mohamed, “A novel model-free deep reinforcement learning framework for energy management of a pv integrated energy hub,” *IEEE Transactions on Power Systems*, vol. 38, no. 5, pp. 4840–4852, 2022.
- [17] K. Ren, J. Liu, Z. Wu, X. Liu, Y. Nie, and H. Xu, “A data-driven drl-based home energy management system optimization framework considering uncertain household parameters,” *Applied Energy*, vol. 355, p. 122258, 2024.
- [18] W. Shi, D. Zhang, X. Han, X. Wang, T. Pu, and W. Chen, “Coordinated operation of active distribution network, networked microgrids, and electric vehicle: A multi-agent ppo optimization method,” *CSEE Journal of Power and Energy Systems*, 2023.
- [19] Y. Zhang, J. Hu, G. Min, and X. Chen, “Scalable and privacy-preserving distributed energy management for multimicrogrid,” *IEEE Transactions on Industrial Informatics*, 2024.
- [20] H. Du, Z. Li, D. Niyato, J. Kang, Z. Xiong, H. Huang, and S. Mao, “Diffusion-based Reinforcement Learning for Edge-enabled AI-Generated Content Services,” Mar. 2023. [Online]. Available: <https://arxiv.org/abs/2303.13052v3>
- [21] Y. Zhang, Z. Mei, X. Wu, H. Jiang, J. Zhang, and W. Gao, “Two-Step Diffusion Policy Deep Reinforcement Learning Method for Low-Carbon Multi-Energy Microgrid Energy Management,” *IEEE Transactions on Smart Grid*, vol. 15, no. 5, pp. 4576–4588, Sep. 2024, conference Name: IEEE Transactions on Smart Grid. [Online]. Available: <https://ieeexplore.ieee.org/document/10529228?arnumber=10529228>
- [22] T. Haarnoja, A. Zhou, P. Abbeel, and S. Levine, “Soft actor-critic: Off-policy maximum entropy deep reinforcement learning with a stochastic actor,” in *International conference on machine learning*. PMLR, 2018, pp. 1861–1870.
- [23] Y. Shen, M. J. Tobia, T. Sommer, and K. Obermayer, “Risk-sensitive reinforcement learning,” *Neural computation*, vol. 26, no. 7, pp. 1298–1328, 2014.
- [24] T. Enders, J. Harrison, and M. Schiffer, “Risk-sensitive soft actor-critic for robust deep reinforcement learning under distribution shifts,” *arXiv preprint arXiv:2402.09992*, 2024.
- [25] H. Eriksson and C. Dimitrakakis, “Epistemic risk-sensitive reinforcement learning,” *arXiv preprint arXiv:1906.06273*, 2019.
- [26] X. Ma, J. Chen, L. Xia, J. Yang, Q. Zhao, and Z. Zhou, “Dsac: Distributional soft actor-critic for risk-sensitive reinforcement learning,” *Journal of Artificial Intelligence Research*, vol. 83, 2025.
- [27] J. Ho, A. Jain, and P. Abbeel, “Denoising diffusion probabilistic models,” *Advances in neural information processing systems*, vol. 33, pp. 6840–6851, 2020.
- [28] B. Huang and J. Wang, “Deep-reinforcement-learning-based capacity scheduling for pv-battery storage system,” *IEEE Transactions on Smart Grid*, vol. 12, no. 3, pp. 2272–2283, 2020.